Journal of Sound and Vibration 331 (2012) 4807–4824

Contents lists available at SciVerse ScienceDirect

Journal of Sound and Vibration

journal homepage: www.elsevier.com/locate/jsvi

Modal properties and stability of centrifugal pendulum vibration absorber systems with equally spaced, identical absorbers

Chengzhi Shi [a], Robert G. Parker [b,*]

[a] University of Michigan-Shanghai Jiao Tong University Joint Institute, Shanghai Jiao Tong University, Shanghai 200240, PR China
[b] State Key Laboratory for Mechanical Systems and Vibration, University of Michigan-Shanghai Jiao Tong University Joint Institute, Shanghai Jiao Tong University, Shanghai 200240, PR China

ARTICLE INFO

Article history:
Received 10 February 2012
Received in revised form
11 May 2012
Accepted 11 May 2012
Handling Editor: L.N. Virgin
Available online 21 June 2012

ABSTRACT

This work develops an analytical model of centrifugal pendulum vibration absorber systems with equally spaced, identical absorbers and uses it to investigate the structure of the modal vibration properties. The planar model admits two translational and one rotational degrees-of-freedom for the rotor and a single arclength degree-of-freedom for each absorber. The gyroscopic effects from rotor rotation are taken into account. Examination of the associated eigenvalue problem reveals well-defined structure of the vibration modes resulting from the cyclic symmetry of the absorbers. The vibration modes are classified into rotational, translational, and absorber modes. Characteristics of each mode type are analytically proved. The effects of the absorber tuning order on the modes are derived. The critical speeds and flutter instability of the system are studied numerically and analytically.

1. Introduction

Centrifugal pendulum vibration absorbers (CPVAs) are used to reduce rotational vibrations in rotating machinery. For example, CPVAs are used in internal combustion engines and helicopter rotors. The natural frequency of an individual CPVA is designed to be proportional to the rotation speed of the rotor with the result that rotor vibration at a particular order of rotation speed is reduced at every speed.

Taylor [1] showed the effectiveness of CPVAs used in radial aircraft engines. Newland [2] studied nonlinear CPVAs using a piecewise linear approximation to the pendulum torque–amplitude describing function. Denman [3] studied different CPVA paths and found that an epicycloidal path is better than circular because the period of the oscillating pendulum is equal to the period of the excitation torque even for large amplitude oscillations. The dynamic response and stability of the CPVA system was studied by perturbation theory [4–7]. The non-unison dynamic responses of the system with multiple CPVAs was investigated using bifurcation analysis [8,9]. Experimental testing was conducted as well [10,11]. Theoretical and experimental results were compared with good agreement [12,13].

Besides counteracting the torsional vibration, CPVAs might also be used to reduce translational vibration, for example in the automotive engine shake or helicopter rotor problems. In a rare work including rotor translation, Cronin [14] showed the shake reduction that occurs in four cylinder, four-cycle engines using CPVAs. Cronin's model included an

* Corresponding author at: State Key Laboratory for Mechanical Systems and Vibration, University of Michigan-Shanghai Jiao Tong University Joint Institute, Shanghai Jiao Tong University, Shanghai 200240, PR China. Tel.: +86 21 3420 6356; fax: +86 21 3420 6525.
E-mail address: rparker@sjtu.edu.cn (R.G. Parker).

0022-460X/$ - see front matter © 2012 Elsevier Ltd. All rights reserved.
http://dx.doi.org/10.1016/j.jsv.2012.05.018

engine block, pistons, and connecting rods as well as a rotor (crankshaft) and absorbers. The linear model derived by Cronin neglected the stiffness of the crankshaft bearings, and some terms are missing in the linearized equations. Cronin did not determine the natural frequencies or modal properties. Bauchau et al. [15] showed significant reduction in hub translational displacement for the Sikorsky UH-60 helicopter rotor by applying CPVAs.

This work derives the nonlinear, gyroscopic equations of motion for a CPVA system with rotor translation, linearizes the model, and investigates the natural frequencies, vibration modes, and stability of the CPVA system with equally spaced, identical absorbers. We identify and mathematically prove the well-defined vibration mode structure that results from the cyclic symmetry. There are only three mode types: rotational, translational, and absorber modes. The two differing cases of unity and non-unity CPVA tuning must be examined separately. This vibration mode structure is similar to that of gyroscopic planetary gear systems [16–18]. Such modal properties can be used to interpret observed vibrations and for nonlinear response analysis using, for instance, perturbation methods and bifurcation theory.

As a gyroscopic system, CPVA systems experience critical speeds and flutter instability. Relevant stability conditions are derived analytically.

2. Mathematical model

The CPVA system model consists of N identical absorbers mounted on a rotor at equally spaced angles. The rotor has two translational and one rotational degrees-of-freedom. All absorbers are bifilar absorbers [3] that work like a point mass moving on a specified path cut into the rotor. Hence, the moments of inertia of the absorbers are not relevant. The bifilar absorbers are suspended by sets of rollers whose moments of inertia are neglected in this work. The study by Monroe et al. [19] considers the effects of these rollers. Because the natural frequencies of the absorbers are, by design, proportional to the rotor speed, the CPVA system is an order-tuned system that performs its vibration absorption function at every rotor speed, assuming the excitation frequency is a multiple of rotor speed. The proportionality coefficient between rotor speed and individual absorber natural frequency is defined as the tuning order of the absorbers.

Fig. 1 shows the bases and coordinates used. $\{\mathbf{E}_1,\mathbf{E}_2\}$ is the fixed basis. The corotational basis $\{\mathbf{e}_1^0,\mathbf{e}_2^0\}$ is fixed to the rotor and rotates with angular speed $\Omega+\dot{\mu}_r$, where Ω is the nominal angular speed of the rotor and μ_r is the rotational vibration of the rotor. The coordinates x_r and y_r of the rotor are assigned to translations along $\mathbf{e}_1^0$ and $\mathbf{e}_2^0$. The basis $\{\hat{\mathbf{e}}_1^i,\hat{\mathbf{e}}_2^i\}$, also fixed to the rotor, is defined such that $\hat{\mathbf{e}}_1^i$ points from the center of the rotor to the pivot of the ith absorber. l denotes the distance between the center of the rotor and the pivot of each absorber. The angles β_i describe the pivot position of the ith absorber. The basis $\{\hat{\mathbf{e}}_1^i,\hat{\mathbf{e}}_2^i\}$ is corotational with the ith absorber, with $\hat{\mathbf{e}}_1^i$ directed from the pivot to the absorber mass. The coordinate s_i describes the deviation from the nominal position ($\xi_i=0$) along the path for each absorber. $r(s_i)$ is the absorber radius. For absorbers with a general path of travel, $r(s_i)$ and the deviation angle $\xi_i(s_i)$ are functions of s_i. When the path of each absorber is circular, the radius r is constant and the deviation angle $\xi_i=s_i/r$. Throughout the paper, the index i ranges from 1 to N.

The natural frequency of an absorber viewed as a single degree-of-freedom with small angular motion attached to a rotor spinning at constant speed Ω is $\Omega\sqrt{l/r(0)}$, where $r(0)$ denotes the radius of the absorber at its nominal position. The tuning order is $n=\sqrt{l/r(0)}$.

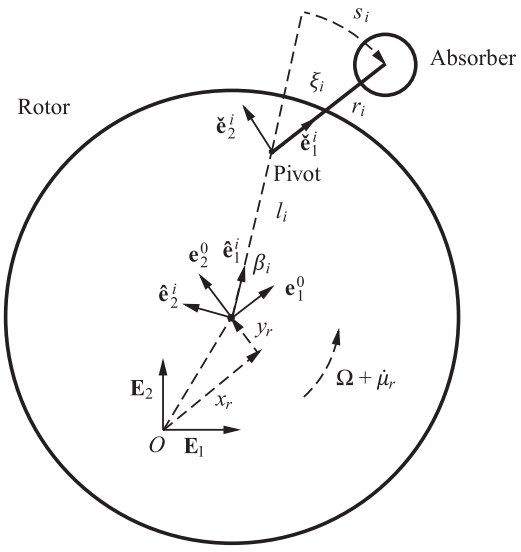

Fig. 1. Bases and coordinates used in the CPVA system.

2.1. Equations of motion

The kinetic and potential energies are

$$T = \frac{1}{2} m_r \dot{\mathbf{r}}_r \cdot \dot{\mathbf{r}}_r + \frac{1}{2} J_r (\Omega + \dot{\mu}_r)^2 + \frac{1}{2} m \sum_{i=1}^{N} \dot{\mathbf{r}}_a^i \cdot \dot{\mathbf{r}}_a^i, \tag{1a}$$

$$V = \tfrac{1}{2} k_r (x_r^2 + y_r^2), \tag{1b}$$

where m_r is the mass of the rotor, J_r is the moment of inertia of the rotor about its center, k_r is the translational stiffness of the rotor support bearings, and m is the mass of each absorber. $\mathbf{r}_r$ and $\mathbf{r}_a^i$ are the position vectors of the rotor center and the ith absorber relative to the fixed origin O.

The angular speeds of the three defined rotating bases, $\{\mathbf{e}_1^0, \mathbf{e}_2^0\}$, $\{\hat{\mathbf{e}}_1^i, \hat{\mathbf{e}}_2^i\}$, and $\{\check{\mathbf{e}}_1 i, \hat{\mathbf{e}}_2^i\}$, are

$$\omega^0 = \hat{\omega}^i = \Omega + \dot{\mu}_r, \tag{2a}$$

$$\check{\omega}^i = \Omega + \dot{\mu}_r + \xi_i' \dot{s}_i, \tag{2b}$$

where $(\cdot)'$ denotes the partial derivative with respect to s_i. The position vectors of the rotor and the absorbers are

$$\mathbf{r}_r = x_r \mathbf{e}_1^0 + y_r \mathbf{e}_2^0, \tag{3a}$$

$$\mathbf{r}_a^i = x_r \mathbf{e}_1^0 + y_r \mathbf{e}_2^0 + l \hat{\mathbf{e}}_1^i + r \hat{\mathbf{e}}_1^i. \tag{3b}$$

The translational velocities of the rotor and the absorbers are

$$\dot{\mathbf{r}}_r = [\dot{x}_r - y_r(\Omega + \dot{\mu}_r)]\mathbf{e}_1^0 + [\dot{y}_r + x_r(\Omega + \dot{\mu}_r)]\mathbf{e}_2^0, \tag{4a}$$

$$\dot{\mathbf{r}}_a^i = [\dot{x}_r - y_r(\Omega + \dot{\mu}_r)]\mathbf{e}_1^0 + [\dot{y}_r + x_r(\Omega + \dot{\mu}_r)]\mathbf{e}_2^0 + l(\Omega + \dot{\mu}_r)\hat{\mathbf{e}}_2^i + r(\Omega + \dot{\mu}_r + \xi_i' \dot{s}_i)\hat{\mathbf{e}}_2^i + r' \dot{s}_i \hat{\mathbf{e}}_1^i. \tag{4b}$$

Substitution of the translational velocities into Eq. (1a) yields the kinetic energy as

$$T = \frac{1}{2} \sum_{i=1}^{N+3} \sum_{j=1}^{N+3} \alpha_{ij}(q_k, t) \dot{q}_i \dot{q}_j + \sum_{i=1}^{N+3} f_i(q_k, t) \dot{q}_i + T_0(q_k, t), \tag{5}$$

where $k = 1, 2, \ldots, N+3$ and q_i denotes elements of the generalized coordinate vector

$$\mathbf{q} = (x_r, y_r, \mu_r, s_1, s_2, \ldots, s_N)^T. \tag{6}$$

The coefficients α_{ij} are elements of an $(N+3) \times (N+3)$ symmetric matrix given by

$$\alpha_{11} = m_r + Nm, \tag{7a}$$

$$\alpha_{12} = 0, \tag{7b}$$

$$\alpha_{13} = -m_r y_r - m \sum_{i=1}^{N} \left[l \sin(\beta_i) + r \sin\left(\beta_i + \frac{s_i}{r}\right) + y_r \right], \tag{7c}$$

$$\alpha_{1\{i+3\}} = m[r' \cos(\beta_i + \xi_i) - r\xi_i' \sin(\beta_i + \xi_i)], \tag{7d}$$

$$\alpha_{22} = m_r + Nm, \tag{7e}$$

$$\alpha_{23} = m_r x_r + m \sum_{i=1}^{N} \left[l \cos(\beta_i) + r \cos\left(\beta_i + \frac{s_i}{r}\right) + x_r \right], \tag{7f}$$

$$\alpha_{2\{i+3\}} = m[r' \sin(\beta_i + \xi_i) + r\xi_i' \cos(\beta_i + \xi_i)], \tag{7g}$$

$$\alpha_{33} = J_r + m_r(x_r^2 + y_r^2) + m \sum_{i=1}^{N} \{l^2 + r^2 + x_r^2 + y_r^2 + 2l[r \cos(\xi_i) + x_r \cos(\beta_i) + y_r \sin(\beta_i)] + 2r[x_r \cos(\beta_i + \xi_i) + y_r \sin(\beta_i + \xi_i)]\}, \tag{7h}$$

$$\alpha_{3\{i+3\}} = m\{r'[l \cos(\xi_i) + x_r \cos(\beta_i + \xi_i) + y_r \sin(\beta_i + \xi_i) + r] + r\xi_i'[l \sin(\xi_i) + x_r \sin(\beta_i + \xi_i) - y_r \cos(\beta_i + \xi_i)]\}, \tag{7i}$$

$$\alpha_{\{i+3\}\{i+3\}} = m(r'^2 + r^2 \xi_i'^2). \tag{7j}$$

The coefficients f_i and T_0 are

$$f_1 = \Omega \alpha_{13}, \quad f_2 = \Omega \alpha_{23}, \quad f_3 = \Omega \alpha_{33}, \quad f_{\{i+3\}} = \Omega \alpha_{3\{i+3\}}, \tag{8a}$$

$$T_0 = \tfrac{1}{2} \Omega^2 \alpha_{33}. \tag{8b}$$

Substitution of the kinetic and potential energies into Lagrange's equations yields the nonlinear equations of motion

$$\sum_{i=1}^{N+3}\left[\alpha_{ki}\ddot{q}_i-\sum_{j=1}^{N+3}\frac{1}{2}\frac{\partial\alpha_{ij}}{\partial q_k}\dot{q}_i\dot{q}_j+\left(\sum_{p=1}^{N+3}\frac{\partial\alpha_{ki}}{\partial q_p}\dot{q}_p+\frac{\partial\alpha_{ki}}{\partial t}\right)\dot{q}_i-\frac{\partial f_i}{\partial q_k}\dot{q}_i\right]+\sum_{p=1}^{N+3}\frac{\partial f_k}{\partial q_p}\dot{q}_p+\frac{\partial f_k}{\partial t}-\frac{\partial T_0}{\partial q_k}+\frac{\partial V}{\partial q_k}=Q_k,\quad k=1,2,\ldots,N+3, \tag{9}$$

where the Q_k are generalized forces given by

$$Q_1=F_x(t),\quad Q_2=F_y(t),\quad Q_3=T_r(t),\quad Q_{\{i+3\}}=0. \tag{10}$$

$F_x(t)$, $F_y(t)$, and $T_r(t)$ are the forces and torque applied to the rotor.

2.2. Linearization

The full nonlinear equations of motion in Eq. (9) are linearized for small motions about the nominal position $\mathbf{q}=\mathbf{0}$ induced by constant rotation. This results in

$$\mathbf{M}\ddot{\mathbf{q}}+\Omega\mathbf{G}\dot{\mathbf{q}}+(\mathbf{K}_b-\Omega^2\mathbf{K}_\Omega)\mathbf{q}=\mathbf{F}+\mathbf{H}, \tag{11}$$

where the mass matrix $\mathbf{M}$, the gyroscopic matrix $\mathbf{G}$, and the stiffness matrices $\mathbf{K}_b$ and $\mathbf{K}_\Omega$ are

$$\mathbf{M}=\begin{pmatrix}\mathbf{M}_r & \mathbf{M}_{ra}\\ \text{symmetric} & \mathbf{M}_a\end{pmatrix}, \tag{12a}$$

$$\mathbf{G}=2\begin{pmatrix}\mathbf{G}_r & \mathbf{G}_{ra}\\ \text{skew-symmetric} & \mathbf{0}_{N\times N}\end{pmatrix}, \tag{12b}$$

$$\mathbf{K}_b=\begin{pmatrix}\mathbf{K}_{rb} & \mathbf{0}_{3\times N}\\ \text{symmetric} & \mathbf{0}_{N\times N}\end{pmatrix}, \tag{12c}$$

$$\mathbf{K}_\Omega=\begin{pmatrix}\mathbf{K}_r & \mathbf{K}_{ra}\\ \text{symmetric} & \mathbf{K}_a\end{pmatrix}. \tag{12d}$$

The sub-matrices in Eq. (12) are

$$\mathbf{M}_r=\begin{pmatrix}m_r+Nm & 0 & -m(l+r)\sum_{i=1}^{N}\sin\beta_i\\ & m_r+Nm & m(l+r)\sum_{i=1}^{N}\cos\beta_i\\ \text{symmetric} & & J_r+Nm(l+r)^2\end{pmatrix}, \tag{13a}$$

$$\mathbf{M}_{ra}=\begin{pmatrix}-m\sin\beta_1 & -m\sin\beta_2 & \cdots & -m\sin\beta_N\\ m\cos\beta_1 & m\cos\beta_2 & \cdots & m\cos\beta_N\\ m(l+r) & m(l+r) & \cdots & m(l+r)\end{pmatrix}, \tag{13b}$$

$$\mathbf{M}_a=\operatorname{diag}(\underbrace{m,m,\ldots,m}_{N}), \tag{13c}$$

$$\mathbf{G}_r=\begin{pmatrix}0 & -(m_r+Nm) & -m(l+r)\sum_{i=1}^{N}\cos\beta_i\\ & 0 & -m(l+r)\sum_{i=1}^{N}\sin\beta_i\\ \text{skew-symmetric} & & 0\end{pmatrix}, \tag{13d}$$

$$\mathbf{G}_{ra}=\begin{pmatrix}-m\cos\beta_1 & -m\cos\beta_2 & \cdots & -m\cos\beta_N\\ -m\sin\beta_1 & -m\sin\beta_2 & \cdots & -m\sin\beta_N\\ 0 & 0 & \cdots & 0\end{pmatrix}, \tag{13e}$$

$$\mathbf{K}_{rb}=\operatorname{diag}(k_r,k_r,0), \tag{13f}$$

$$\mathbf{K}_r=\operatorname{diag}(m_r+Nm,m_r+Nm,0), \tag{13g}$$

$$\mathbf{K}_{ra}=\begin{pmatrix} -m\sin\beta_1 & -m\sin\beta_2 & \cdots & -m\sin\beta_N \\ m\cos\beta_1 & m\cos\beta_2 & \cdots & m\cos\beta_N \\ 0 & 0 & \cdots & 0 \end{pmatrix}, \tag{13h}$$

$$\mathbf{K}_a=\mathrm{diag}(\underbrace{-ml/r,-ml/r,\ldots,-ml/r}_{N}). \tag{13i}$$

The operator diag$(\cdot)$ forms a diagonal matrix with the elements listed. The external force $\mathbf{F}$ and the constant centripetal acceleration term $\mathbf{H}$ caused by the angular speed of the rotor are

$$\mathbf{F}=(F_x(t),F_y(t),T_r(t),\underbrace{0,0,\ldots,0}_{N})^T, \tag{14a}$$

$$\mathbf{H}=\Omega^2\left(m(l+r)\sum_{i=1}^{N}\cos\beta_i,m(l+r)\sum_{i=1}^{N}\sin\beta_i,\underbrace{0,0,\ldots,0}_{N+1}\right)^T, \tag{14b}$$

where $(\cdot)^T$ denotes the transpose of a matrix or vector. $\mathbf{H}$ vanishes for equally spaced, identical absorbers.

The linearized equations of motion in Eq. (11) apply for general absorber paths that are locally circular around their nominal positions. This includes circular, epicycloidal, and cycloidal paths, the three types in practical use [3].

The eigenvalue problem of Eq. (11) is

$$\lambda^2\mathbf{M}\boldsymbol{\phi}+\lambda\Omega\mathbf{G}\boldsymbol{\phi}+(\mathbf{K}_b-\Omega^2\mathbf{K}_\Omega)\boldsymbol{\phi}=\mathbf{0}. \tag{15}$$

The mass matrix $\mathbf{M}$ and the stiffness matrices $\mathbf{K}_b$ and $\mathbf{K}_\Omega$ are symmetric, and the gyroscopic matrix $\mathbf{G}$ is skew-symmetric. The eigenvalue problem in Eq. (15) is a standard gyroscopic eigenvalue problem [20]. The eigenvalues and eigenvectors are complex-valued and always appear as complex conjugate pairs. The natural frequencies are defined as $\omega=|\mathrm{Im}(\lambda)|$, where $\mathrm{Im}(\lambda)$ denotes the imaginary part of λ.

3. Vibration mode structure

Numerical experiments illustrate the modal properties of CPVA systems. The parameters are given in Table 1. Table 2 gives the numerical natural frequencies from Eq. (15) at 2000 rpm (209.44 rad/s). Each natural frequency listed corresponds

Table 1
Parameters of CPVA example systems.

Parameter	Non-unity tuning	Unity tuning
Rotor mass, m_r (kg)	11	
Rotor inertia, J_r (kg m^2)	0.2	
Absorber mass, m (kg)	0.9	
Distance between center and pivot, l (m)	0.04	0.01
Absorber radius, r (m)	0.01	
Rotor translational stiffness, k_r (N/m)	1×10^9	

Table 2
Natural frequencies, ω (rad/s), for CPVA systems with 3, 4, 5, and 6 equally spaced, identical absorbers at rotor angular speed $\Omega=2000$ rpm (209.44 rad/s). The system parameters are given in Table 1. Multiplicities are shown in parentheses.

Mode type	$N=3$		$N=4$		$N=5$		$N=6$	
	$n\neq1$	$n=1$	$n\neq1$	$n=1$	$n\neq1$	$n=1$	$n\neq1$	$n=1$
Rotational	0	0	0	0	0	0	0	0
	425.89	210.00	428.20	210.19	430.50	210.38	432.79	210.57
Translational	418.63	209.34	418.54	209.31	418.46	209.27	418.37	209.24
	418.88	209.44	418.87	209.44	418.87	209.44	418.87	209.44
	8813.9	8813.0	8661.5	8660.4	8516.9	8515.4	8379.3	8377.6
	9186.7	9186.0	9021.2	9020.2	8864.2	8863.0	8715.1	8713.8
Absorber	N/A	N/A	418.88	209.44	418.88 (2)	209.44 (2)	418.88 (3)	209.44 (3)

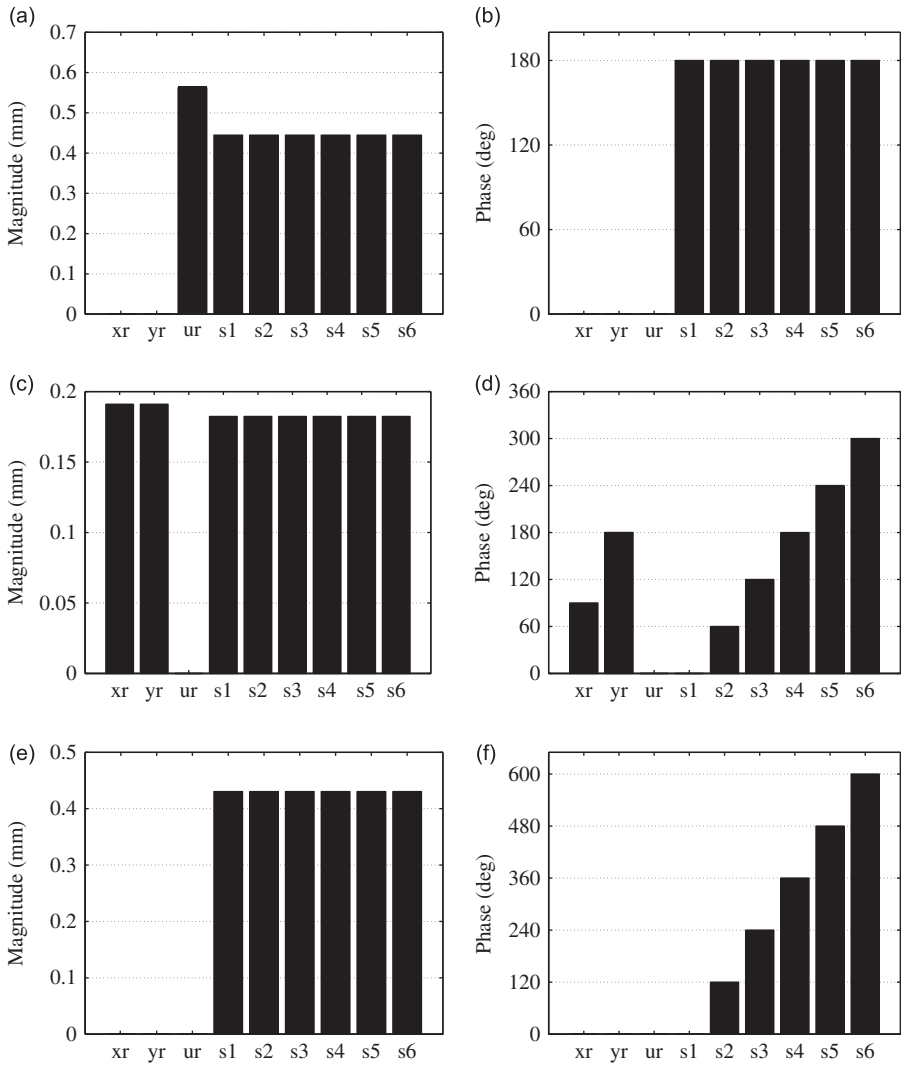

Fig. 2. Structured vibration modes of the CPVA system with six equally spaced, identical absorbers and the system parameters given in Table 1. The horizontal axis labels denote the system degrees-of-freedom. (a) Rotational mode magnitude, $\lambda = \mathrm{j}432.79$ rad/s. (b) Rotational mode phase, $\lambda = \mathrm{j}432.79$ rad/s. (c) Translational mode magnitude, $\lambda = \mathrm{j}8715.1$ rad/s. (d) Translational mode phase, $\lambda = \mathrm{j}8715.1$ rad/s. (e) Absorber mode magnitude, $\lambda = \mathrm{j}418.88$ rad/s. $k=2$. (f) Absorber mode phase, $\lambda = \mathrm{j}418.88$ rad/s. $k=2$.

to a pair of complex conjugate eigenvalues. The corresponding mode shapes reveal only three mode types: rotational modes (Fig. 2(a) and (b)), translational modes (Fig. 2(c) and (d)), and absorber modes (Fig. 2(e) and (f)). The rotational modes have no translation but only rotation of the rotor. The translational modes have no rotation but only translation of the rotor. The absorber modes have no motion in the rotor; only the absorbers move. Absorber modes exist only for $N \geq 4$. Both non-unity and unity tuning cases are studied. For the unity tuning case, one pair of translational modes has zero translation of the rotor for any rotor speed. The associated pair of eigenvalues is degenerate with the pair of absorber mode eigenvalues.

3.1. Non-unity tuning

We first consider CPVA systems with absorbers whose tuning order is not unity. The three types of vibration modes are discussed separately.

3.1.1. Rotational modes

Based on the numerical experiments, rotational modes are presumed to have zero rotor translation and all the absorbers have identical motions. Accordingly, the proposed eigenvector for the rotational modes is

$$\boldsymbol{\phi} = (0, 0, \mu_r, \underbrace{s, s, \ldots, s}_{N})^T. \tag{16}$$

Substitution of Eq. (16) into the eigenvalue problem in Eq. (15) yields

$$-\lambda^2\left[m(l+r)\mu_r\sum_{i=1}^{N}\sin\beta_i+ms\sum_{i=1}^{N}\sin\beta_i\right]-2\lambda\Omega\left[m(l+r)\mu_r\sum_{i=1}^{N}\cos\beta_i+ms\sum_{i=1}^{N}\cos\beta_i\right]+\Omega^2 ms\sum_{i=1}^{N}\sin\beta_i=0, \tag{17a}$$

$$\lambda^2\left[m(l+r)\mu_r\sum_{i=1}^{N}\cos\beta_i+ms\sum_{i=1}^{N}\cos\beta_i\right]-2\lambda\Omega\left[m(l+r)\mu_r\sum_{i=1}^{N}\sin\beta_i+ms\sum_{i=1}^{N}\sin\beta_i\right]-\Omega^2 ms\sum_{i=1}^{N}\cos\beta_i=0, \tag{17b}$$

$$\lambda^2\{[J_r+Nm(l+r)^2]\mu_r+Nm(l+r)s\}=0, \tag{17c}$$

$$\lambda^2[(l+r)\mu_r+s]+\frac{l}{r}\Omega^2 s=0. \tag{17d}$$

The N equations in Eq. (15) for the individual absorber motions s_i all yield Eq. (17d), so Eq. (15) generates only the four equations shown in Eq. (17). The equally spaced absorbers have the property that $\sum_{i=1}^{N}\cos\beta_i=\sum_{i=1}^{N}\sin\beta_i=0$ for $N>1$. Therefore, the equations that govern the translational motions in Eqs. (17a) and (17b) vanish.

Writing Eqs. (17c) and (17d) in matrix form yields

$$\lambda^2\begin{pmatrix}\frac{J_r}{Nm}+(l+r)^2 & l+r\\ l+r & 1\end{pmatrix}\begin{pmatrix}\mu_r\\ s\end{pmatrix}+\Omega^2\begin{pmatrix}0 & 0\\ 0 & \frac{l}{r}\end{pmatrix}\begin{pmatrix}\mu_r\\ s\end{pmatrix}=\mathbf{0}. \tag{18}$$

Eq. (18) is a 2×2 self-adjoint eigenvalue problem. From each of the two eigensolutions of Eq. (18), a full system rotational mode is constructed from Eq. (16). Thus, there are exactly two pairs of complex conjugate rotational mode eigensolutions.

The characteristic equation of Eq. (18) is

$$\left\{J_r\lambda^2+[J_r+Nm(l+r)^2]\frac{l}{r}\Omega^2\right\}\lambda^2=0. \tag{19}$$

One pair of complex conjugate rotational mode eigenvalues is

$$\lambda_{1,2}=\pm \mathrm{j}\Omega\sqrt{\left[1+\frac{Nm(l+r)^2}{J_r}\right]\frac{l}{r}}, \tag{20}$$

where $\mathrm{j}=\sqrt{-1}$. This pair of rotational mode eigenvalues is purely imaginary for any non-zero rotor speed. For these $\lambda_{1,2}$, solution of Eq. (17c) or (17d) gives

$$\mu_r=-\frac{Nm(l+r)}{J_r+Nm(l+r)^2}s. \tag{21}$$

Hence, the associated rotational mode eigenvector is

$$\boldsymbol{\phi}=s\left(0,0,-\frac{Nm(l+r)}{J_r+Nm(l+r)^2},\underbrace{1,1,\ldots,1}_{N}\right)^T. \tag{22}$$

All the absorbers move in-phase with equal amplitude while the rotor moves 180° out-of-phase with the absorbers (Fig. 2(a) and (b)). Because all degrees of freedom are either in-phase or exactly out-of-phase and so achieve their extreme values simultaneously, the rotational modes are standing wave modes [21].

The other pair of rotational mode eigenvalues is zero, and the associated rigid body mode is

$$\boldsymbol{\phi}=(0,0,\mu_r,\underbrace{0,0,\ldots,0}_{N})^T, \tag{23}$$

which has only rotor rotation.

Anticipating subsequent results for the other mode types, the rotational mode eigenvector can be written as

$$\boldsymbol{\phi}=(0,0,\mu_r,se^{\mathrm{j}k\beta_1},se^{\mathrm{j}k\beta_2},\ldots,se^{\mathrm{j}k\beta_N})^T, \tag{24}$$

where $k=0$. The parameter k is the phase index of the vibration mode [22]. The phase index will be used to identify the mode type.

3.1.2. Translational modes

The translational modes have the properties that: the rotation of the rotor is zero, the translations of the rotor are related by $y_r=\mathrm{j}x_r$, and the motions of the absorbers can be expressed as $s_i=se^{\mathrm{j}\beta_i}$. The proposed eigenvector for the translational modes is therefore

$$\boldsymbol{\phi}=(x_r,\mathrm{j}x_r,0,se^{\mathrm{j}\beta_1},se^{\mathrm{j}\beta_2},\ldots,se^{\mathrm{j}\beta_N})^T. \tag{25}$$

Substitution of Eq. (25) into Eq. (15) gives

$$\lambda^2\left[(m_r+Nm)x_r-ms\sum_{i=1}^{N}e^{\mathrm{j}\beta_i}\sin\beta_i\right]-2\lambda\Omega\left[\mathrm{j}(m_r+Nm)x_r+ms\sum_{i=1}^{N}e^{\mathrm{j}\beta_i}\cos\beta_i\right]+k_rx_r-\Omega^2\left[(m_r+Nm)x_r-ms\sum_{i=1}^{N}e^{\mathrm{j}\beta_i}\sin\beta_i\right]=0, \tag{26a}$$

$$\lambda^2\left[\mathrm{j}(m_r+Nm)x_r-ms\sum_{i=1}^{N}e^{\mathrm{j}\beta_i}\cos\beta_i\right]+2\lambda\Omega\left[(m_r+Nm)x_r-ms\sum_{i=1}^{N}e^{\mathrm{j}\beta_i}\sin\beta_i\right]+jk_rx_r-\Omega^2\left[\mathrm{j}(m_r+Nm)x_r+ms\sum_{i=1}^{N}e^{\mathrm{j}\beta_i}\cos\beta_i\right]=0, \tag{26b}$$

$$\lambda^2m(l+r)(\mathrm{j}x_r+s)\sum_{i=1}^{N}e^{\mathrm{j}\beta_i}+2\lambda\Omega m(l+r)s\sum_{i=1}^{N}e^{\mathrm{j}\beta_i}=0, \tag{26c}$$

$$\lambda^2m(\mathrm{j}x_r+s)+2\lambda\Omega mx_r+\Omega^2m\left(-\mathrm{j}x_r+\frac{l}{r}s\right)=0. \tag{26d}$$

As for rotational modes, all of the absorber equations in Eq. (15) reduce to a single identical equation (Eq. (26d)). For equally spaced absorbers $\sum_{i=1}^{N}e^{\mathrm{j}\beta_i}=0$ for $N>1$, as proved in the Appendix, so Eq. (26c) governing rotor rotation vanishes. Additionally, $\sum_{i=1}^{N}\sin\beta_i\cos\beta_i=0$ and $\sum_{i=1}^{N}\cos^2\beta_i=\sum_{i=1}^{N}\sin^2\beta_i=N/2$ (see the Appendix). Hence,

$$\sum_{i=1}^{N}e^{\mathrm{j}\beta_i}\sin\beta_i=\mathrm{j}\frac{N}{2},\quad \sum_{i=1}^{N}e^{\mathrm{j}\beta_i}\cos\beta_i=\frac{N}{2}. \tag{27}$$

Substitution of Eq. (27) into Eq. (26a) yields

$$\lambda^2\left[(m_r+Nm)x_r-\frac{\mathrm{j}N}{2}ms\right]-2\lambda\Omega\left[\mathrm{j}(m_r+Nm)x_r+\frac{N}{2}ms\right]+k_rx_r-\Omega^2\left[(m_r+Nm)x_r-\frac{\mathrm{j}N}{2}ms\right]=0. \tag{28}$$

Substitution of Eq. (27) into Eq. (26b) yields Eq. (28) multiplied by $-\mathrm{j}$.

Writing Eqs. (26d) and (28) in matrix form yields

$$\lambda^2\begin{pmatrix}\frac{2m_r}{Nm}+2 & -\mathrm{j}\\ \mathrm{j} & 1\end{pmatrix}\begin{pmatrix}x_r\\ s\end{pmatrix}+2\lambda\Omega\begin{pmatrix}-\mathrm{j}(\frac{2m_r}{Nm}+2) & -1\\ 1 & 0\end{pmatrix}\begin{pmatrix}x_r\\ s\end{pmatrix}+\left[\begin{pmatrix}\frac{2k_r}{Nm} & 0\\ 0 & 0\end{pmatrix}-\Omega^2\begin{pmatrix}\frac{2m_r}{Nm}+2 & -\mathrm{j}\\ \mathrm{j} & -\frac{l}{r}\end{pmatrix}\right]\begin{pmatrix}x_r\\ s\end{pmatrix}=\mathbf{0}. \tag{29}$$

The complex mass and stiffness matrices are Hermitian, and the complex gyroscopic matrix is skew-Hermitian. Eq. (29) is a 2×2 gyroscopic eigenvalue problem that provides four translational mode eigensolutions. These four eigensolutions do not appear as complex conjugate pairs because the matrices in Eq. (29) are complex. The complex conjugate eigensolutions of the above four eigensolutions are given by the complex conjugate of Eq. (29), which is the matrix eigenvalue problem generated by the above process when $\boldsymbol{\phi}$ in Eq. (25) is replaced by its complex conjugate $\overline{\boldsymbol{\phi}}$. Thus, there are exactly four complex conjugate pairs of translational modes.

The characteristic equation of Eq. (29) is

$$\begin{aligned}&(2m_r+Nm)\lambda^4-4\mathrm{j}m_r\Omega\lambda^3+2\left\{k_r+\left[m_r\left(\frac{l}{r}-1\right)+Nm\left(2+\frac{l}{r}\right)\right]\Omega^2\right\}\lambda^2\\&-4\mathrm{j}\left[m_r\frac{l}{r}+Nm\left(1+\frac{l}{r}\right)\right]\Omega^3\lambda+2k_r\frac{l}{r}\Omega^2-\left[2m_r\frac{l}{r}+Nm\left(1+2\frac{l}{r}\right)\right]\Omega^4=0,\end{aligned} \tag{30}$$

which yields the four translational mode eigenvalues.

When the rotor speed $\Omega=0$, Eq. (30) and its complex conjugate are identical. Hence, the translational mode eigenvalues are degenerate with multiplicity two at zero rotor speed. Two of the four translational mode eigenvalues at zero speed are

$$\lambda_{1,2}=\pm\mathrm{j}\sqrt{\frac{2k_r}{2m_r+Nm}}. \tag{31}$$

The other two translational mode eigenvalues are zero.

Considering Eq. (25) and following the pattern established by Eq. (24), any translational mode eigenvector can be written as

$$\boldsymbol{\phi}=(x_r,\mathrm{j}x_r,0,se^{\mathrm{j}k\beta_1},se^{\mathrm{j}k\beta_2},\ldots,se^{\mathrm{j}k\beta_N})^T, \tag{32}$$

where the phase index $k=1$. For the complex conjugate eigenvector $\overline{\boldsymbol{\phi}}$, the form in Eq. (32) still holds except $x_r\to\overline{x}_r$, $s\to\overline{s}$, and $k=-1$. For equally spaced absorbers, the phase index $k=-1$ is equivalent to $k=N-1$. Hence, the phase indices of the translational modes are $k=1,N-1$.

Eq. (28) gives

$$x_r = \mathrm{j}\frac{Nm}{2}\left[m_r + Nm + \frac{k_r}{(\lambda - \mathrm{j}\Omega)^2}\right]^{-1} s. \tag{33}$$

Thus, for purely imaginary eigenvalues, x_r and s in Eq. (25) are 90° out-of-phase and so are the coordinates x_r and s_1 for equally spaced $\beta_i = 2\pi(i-1)/N$.

Because the translational modes are complex, there are phase differences (evident in Eq. (32)) between the various degrees-of-freedom when the system is in free vibration of one of these modes. The two translational coordinates move with equal amplitude and 90° out-of-phase. All the absorbers move with equal amplitude, and the absorber phases increase sequentially by 360°/N (Fig. 2(c) and (d)). These features indicate that the translational modes are traveling wave modes [21].

3.1.3. Absorber modes

The absorber modes have the property that the translations and the rotation of the rotor are zero. Thus, the proposed absorber mode eigenvector is

$$\boldsymbol{\phi} = (0,0,0,s_1,s_2,\ldots,s_N)^T. \tag{34}$$

Substitution of Eq. (34) into Eq. (15) gives

$$-\lambda^2 \sum_{i=1}^{N} s_i \sin\beta_i - 2\lambda\Omega \sum_{i=1}^{N} s_i \cos\beta_i + \Omega^2 \sum_{i=1}^{N} s_i \sin\beta_i = 0, \tag{35a}$$

$$\lambda^2 \sum_{i=1}^{N} s_i \cos\beta_i - 2\lambda\Omega \sum_{i=1}^{N} s_i \sin\beta_i - \Omega^2 \sum_{i=1}^{N} s_i \cos\beta_i = 0, \tag{35b}$$

$$(l+r)\sum_{i=1}^{N} s_i = 0, \tag{35c}$$

$$\left(\lambda^2 + \frac{l}{r}\Omega^2\right) s_i = 0, \quad i = 1,2,\ldots,N. \tag{35d}$$

To satisfy Eq. (35c)

$$\sum_{i=1}^{N} s_i = 0. \tag{36}$$

Because $s_i \neq 0$ for all i, Eq. (35d) gives the only possible pair of complex conjugate absorber mode eigenvalues as

$$\lambda = \pm \mathrm{j}\Omega\sqrt{\frac{l}{r}} = \pm \mathrm{j}\Omega n, \tag{37}$$

where $n = \sqrt{l/r}$ is the tuning order of the absorbers. While there is a single pair of absorber mode eigenvalues, the multiplicity of these eigenvalues is $N-3$, as discussed subsequently. The absorber mode eigenvalues are purely imaginary for any non-zero rotor speed.

Substitution of $\lambda = \mathrm{j}\Omega n$ into Eqs. (35a) and (35b) yields

$$(n^2+1)\sum_{i=1}^{N} s_i \sin\beta_i - 2\mathrm{j}n \sum_{i=1}^{N} s_i \cos\beta_i = 0, \tag{38a}$$

$$(n^2+1)\sum_{i=1}^{N} s_i \cos\beta_i + 2\mathrm{j}n \sum_{i=1}^{N} s_i \sin\beta_i = 0. \tag{38b}$$

Allowing for complex s_i, it is convenient to write these equations in the complex form

$$\sum_{i=1}^{N} s_i \left[\frac{(n+1)^2}{2} e^{\mathrm{j}\beta_i} - \frac{(n-1)^2}{2} e^{-\mathrm{j}\beta_i}\right] = 0, \tag{39a}$$

$$\sum_{i=1}^{N} s_i \left[\frac{(n+1)^2}{2} e^{\mathrm{j}\beta_i} + \frac{(n-1)^2}{2} e^{-\mathrm{j}\beta_i}\right] = 0. \tag{39b}$$

Further simplification gives

$$(n+1)^2 \sum_{i=1}^{N} s_i e^{\mathrm{j}\beta_i} = 0, \tag{40a}$$

$$(n-1)^2 \sum_{i=1}^{N} s_i e^{-\mathrm{j}\beta_i} = 0. \tag{40b}$$

In this section we have stipulated $n \neq 1$; unity tuning order is treated subsequently. Thus, satisfaction of Eqs. (40a) and (40b) requires

$$\sum_{i=1}^{N} s_i e^{\mathrm{j}\beta_i} = 0, \tag{41a}$$

$$\sum_{i=1}^{N} s_i e^{-\mathrm{j}\beta_i} = 0. \tag{41b}$$

Writing Eqs. (36) and (41) in matrix form yields

$$\mathbf{A}\mathbf{s} = \mathbf{0}, \tag{42a}$$

$$\mathbf{A} = \begin{pmatrix} 1 & 1 & \cdots & 1 \\ e^{\mathrm{j}\beta_1} & e^{\mathrm{j}\beta_2} & \cdots & e^{\mathrm{j}\beta_N} \\ e^{-\mathrm{j}\beta_1} & e^{-\mathrm{j}\beta_2} & \cdots & e^{-\mathrm{j}\beta_N} \end{pmatrix}, \tag{42b}$$

$$\mathbf{s} = (s_1, s_2, \ldots, s_N)^T. \tag{42c}$$

The absorber mode eigenvalue $\lambda = \mathrm{j}\Omega n$ is known from Eq. (37). Solving for the absorber mode eigenvectors is equivalent to solving for the null space of $\mathbf{A}$. To calculate the rank of $\mathbf{A}$, the three rows of $\mathbf{A}$ are written as three N-dimensional vectors. With the property that $\sum_{i=1}^{N} e^{\mathrm{j}k\beta_i} = 0$ for any integer k that is not a multiple of N, as proved in the Appendix, all inner products between the three vectors vanish. Hence, the three rows of $\mathbf{A}$ are mutually orthogonal and independent, the rank of $\mathbf{A}$ is three, the dimension of the null space of $\mathbf{A}$ is $N-3$, and Eq. (42) has $N-3$ independent solutions for $\mathbf{s}$. Anticipating later results, these are numbered as $\mathbf{s}_k$, $k = 2, 3, \ldots, N-2$. These solutions are substituted into Eq. (34) to get $N-3$ complete system absorber modes. Clearly absorber modes exist only for $N \geq 4$. The degenerate eigenvalue $\lambda = \mathrm{j}\Omega n$ has multiplicity $N-3$, because there are $N-3$ independent absorber modes generated by the $\mathbf{s}_k$.

Using the property $\sum_{i=1}^{N} e^{\mathrm{j}k\beta_i} = 0$ for any integer k that is not a multiple of N as derived in the Appendix, the vectors

$$\mathbf{s}_k = (e^{\mathrm{j}k\beta_1}, e^{\mathrm{j}k\beta_2}, \ldots, e^{\mathrm{j}k\beta_N})^T, \quad k = 2, 3, \ldots, N-2 \tag{43}$$

satisfy Eq. (42). These vectors resemble the eigenvectors of circulant system matrices derived for cyclic systems [23]. They provide an orthogonal basis of the null space of $\mathbf{A}$ and are a complete set of solutions of Eq. (42). Hence, the absorber mode eigenvectors are

$$\boldsymbol{\phi}_k = (0, 0, 0, e^{\mathrm{j}k\beta_1}, e^{\mathrm{j}k\beta_2}, \ldots, e^{\mathrm{j}k\beta_N})^T, \quad k = 2, 3, \ldots, N-2. \tag{44}$$

The orthogonal basis also satisfies the orthogonality condition studied by Olson [21] and Ottarsson [24] that is important in the modal decomposition of rotationally periodic systems.

Analogous to Eqs. (24) and (32), the phase indices of the absorber modes are $k = 2, 3, \ldots, N-2$. Expressed as in Eq. (44), the eigenvectors are complex. There is a phase difference of $k \cdot 360^\circ/N$ between each absorber's motion for free vibration in one of these modes. All absorber amplitudes are equal (see Fig. 2(e) and (f), where the phase index $k=2$).

Substitution of $\lambda = -\mathrm{j}\Omega n$ into Eqs. (35a) and (35b) yields, as for $\lambda = \mathrm{j}\Omega n$, Eq. (41), thus also yielding Eq. (42). Like the $\mathbf{s}_k$, the $N-3$ vectors $\bar{\mathbf{s}}_k$ form a complete set of solutions of Eq. (42). The corresponding absorber mode eigenvectors are $\overline{\boldsymbol{\phi}}_k$ (analogous to Eq. (44) for $\lambda = \mathrm{j}\Omega n$). Thus, the eigenvectors $\overline{\boldsymbol{\phi}}_k$ associated with $\lambda = -\mathrm{j}\Omega n$ are the complex conjugate of the eigenvectors $\boldsymbol{\phi}_k$ associated with $\lambda = \mathrm{j}\Omega n$.

Eqs. (36) and (41) are equivalent to

$$\sum_{i=1}^{N} s_i = 0, \quad \sum_{i=1}^{N} s_i \cos\beta_i = 0, \quad \sum_{i=1}^{N} s_i \sin\beta_i = 0. \tag{45}$$

Using these equations, Cooley and Parker [18] derived $N-3$ real-valued solutions for $\mathbf{s}$ as

$$\mathbf{s}_k^{(r)} = (s_1^{(k)}, s_2^{(k)}, s_3^{(k)}, 0, 0, \ldots, 0, \underbrace{1}_{k+3}, 0, 0, \ldots, 0)^T, \quad k = 1, 2, \ldots, N-3, \tag{46}$$

where the quantities $s_1^{(k)}$, $s_2^{(k)}$, and $s_3^{(k)}$ are determined by

$$s_1^{(k)} + s_2^{(k)} + s_3^{(k)} = -1, \tag{47a}$$

$$s_1^{(k)} \cos\beta_1 + s_2^{(k)} \cos\beta_2 + s_3^{(k)} \cos\beta_3 = -\cos\beta_{k+3}, \tag{47b}$$

$$s_1^{(k)} \sin\beta_1 + s_2^{(k)} \sin\beta_2 + s_3^{(k)} \sin\beta_3 = -\sin\beta_{k+3}. \tag{47c}$$

Using these solutions for the s_i in Eq. (34) reveals that there exists a set of $N-3$ independent absorber modes that are real, in contrast to the complex modes in Eqs. (43) and (44). Unlike the absorber modes as expressed in Eq. (44), when the system vibrates freely in one of these real-valued modes, the absorbers all move in-phase or 180° out-of-phase with each

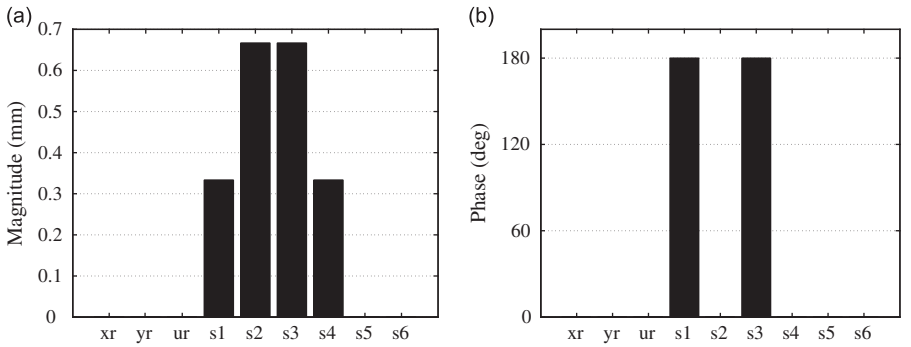

Fig. 3. Real absorber mode of the CPVA system with six equally spaced, identical absorbers and the system parameters given in Table 1. The horizontal axis labels denote the system degrees-of-freedom. (a) Absorber mode magnitude, $\lambda = \mathrm{j}418.88$ rad/s. (b) Absorber mode phase, $\lambda = \mathrm{j}418.88$ rad/s.

other (Fig. 3(b)). The amplitudes of the absorber motions are not equal (Fig. 3(a)), however, as they are in the $\boldsymbol{\phi}_k$ of Eq. (44) (see Fig. 2(e) and (f)). The eigenvector shown in Fig. 3 is a standing wave mode, while the eigenvector displayed by Fig. 2(e) and (f) is a traveling wave mode [21]. The above results show that absorber modes can be treated as either standing or traveling wave modes.

The $N-3$ real-valued $\mathbf{s}_k^{(r)}$ in Eq. (46) are related with the $N-3$ complex-valued $\mathbf{s}_k$ in Eq. (43) by

$$\mathbf{S} = \mathbf{S}^{(r)}\mathbf{R}, \tag{48a}$$

$$\mathbf{R} = \begin{pmatrix} e^{\mathrm{j}2\beta_4} & e^{\mathrm{j}3\beta_4} & \cdots & e^{\mathrm{j}(N-2)\beta_4} \\ e^{\mathrm{j}2\beta_5} & e^{\mathrm{j}3\beta_5} & \cdots & e^{\mathrm{j}(N-2)\beta_5} \\ \vdots & \vdots & \ddots & \vdots \\ e^{\mathrm{j}2\beta_N} & e^{\mathrm{j}3\beta_N} & \cdots & e^{\mathrm{j}(N-2)\beta_N} \end{pmatrix}, \tag{48b}$$

where $\mathbf{S}^{(r)}$ and $\mathbf{S}$ are matrices containing $N-3$ column vectors formed by the real-valued $\mathbf{s}_k^{(r)}$ and the complex-valued $\mathbf{s}_k$, respectively. $\mathbf{R}$ is invertible. Eq. (48) shows that each of the sets of $N-3$ solutions can be written as a linear combination of the other set. Hence, both sets span the null space of $\mathbf{A}$. Therefore, the real and complex-valued sets of absorber modes are equivalent.

3.1.4. Completeness of the vibration mode structure

The CPVA system model has $N+3$ degrees-of-freedom, so there are $N+3$ pairs of complex conjugate vibration modes. The analytical derivation yields two pairs of rotational modes with distinct eigenvalues, four pairs of translational modes with distinct eigenvalues, and one pair of absorber modes with eigenvalue multiplicity $N-3$. The total number of derived rotational, translational, and absorber modes is thus $N+3$ complex conjugate mode pairs. This equals the number of degrees-of-freedom, so the modal description is complete. The CPVA system has only rotational, translational, and absorber modes; no other mode types are possible.

With the excitation $\mathbf{F}$ in Eq. (14) and the eigenvectors of the three mode types in Eqs. (16), (25), and (34), the modal forces $\overline{\boldsymbol{\phi}}^T\mathbf{F}$ are calculated. From these, the rotational modes can be excited only by external rotor torque but not force. The translational modes can be excited only by external rotor force but not torque. No external rotor excitations can excite the absorber modes.

3.2. Unity tuning

The unity tuning case involves $n = \sqrt{l/r} = 1$. In this case, a pair of translational modes has zero translation of the rotor, and the associated pair of eigenvalues is degenerate with the pair of absorber mode eigenvalues. All other vibration mode properties remain the same as for the non-unity tuning case.

To show this, we first note that $\lambda = \mathrm{j}\Omega$ is a solution of the translational mode characteristic equation in Eq. (30) when the tuning order $n = \sqrt{l/r} = 1$. This is degenerate with the absorber mode eigenvalue given in Eq. (37). Substitution of $\lambda = \mathrm{j}\Omega$ and $l/r = 1$ into the translational mode eigenvalue problem in Eq. (29) yields the associated eigenvector as

$$\boldsymbol{\phi} = s(0,0,0,e^{\mathrm{j}\beta_1},e^{\mathrm{j}\beta_2},\ldots,e^{\mathrm{j}\beta_N})^T. \tag{49}$$

Therefore, this translational mode has zero translation of the rotor for any rotor speed. The complex conjugate pair $(\overline{\lambda},\overline{\boldsymbol{\phi}})$ is also a translational mode.

Turning to the absorber modes, Eq. (40b) holds automatically for $n=1$. Eq. (42) becomes

$$\mathbf{B}\mathbf{s} = \mathbf{0}, \tag{50a}$$

$$\mathbf{B}=\begin{pmatrix} 1 & 1 & \cdots & 1 \\ e^{\mathrm{j}\beta_1} & e^{\mathrm{j}\beta_2} & \cdots & e^{\mathrm{j}\beta_N} \end{pmatrix}. \tag{50b}$$

The $N-2$ dimensional solution space for Eq. (50) is spanned by the orthogonal set of solutions consisting of the $\mathbf{s}_k$ in Eq. (43) for $k=2,3,\ldots,N-2$ supplemented by $\mathbf{s}_1$. The full system eigenvector generated by $\mathbf{s}_1$ is the same as Eq. (49). Thus, the additional absorber mode from $\mathbf{s}_1$ and its eigenvalue $\lambda=\mathrm{j}\Omega$ are identical to that just calculated for translational modes with the eigenvector given in Eq. (49).

The question arises whether this mode, which has the form of both Eqs. (25) and (34), should be regarded as a translational mode or an absorber mode. The answer comes from the phase index. The eigenvector in Eq. (49) has a phase index of $k=1$, as in Eq. (32) for translational modes. Thus, this mode is a translational mode. This view maintains separation between the translational mode and the absorber mode eigensolution with which the eigenvalue is degenerate. The alternate view abandons the translational and absorber mode distinction for this eigensolution and simply regards it as degenerate with eigenvalue multiplicity $N-2$.

Thus, for unity tuning a pair of translational modes has zero translation of the rotor, and the associated pair of eigenvalues is degenerate with the pair of absorber mode eigenvalues. As for non-unity tuning, the total number of rotational (2), translational (4), and absorber ($N-3$) mode pairs is identical to the number of degrees-of-freedom, so there are only rotational, translational, and absorber modes.

3.3. Phase indices

The CPVA system with equally spaced, identical absorbers is a cyclically symmetric system. A unique phase index k can be used to describe the characteristic of each vibration mode of such systems [22]. Phase indices for each of rotational, translational, and absorber modes are given above. There is no overlap of phase indices between the three mode types.

Based on the equations of motion in Eq. (11), the net forces and moment that the absorbers exert on the rotor for a particular vibration mode are (with $\mathbf{q}\rightarrow\mathbf{q}e^{\lambda t}$)

$$P_x=m\left[(\lambda^2-\Omega^2)\sum_{i=1}^{N}s_i\sin\beta_i+2\lambda\Omega\sum_{i=1}^{N}s_i\cos\beta_i\right]e^{\lambda t}, \tag{51a}$$

$$P_y=m\left[(-\lambda^2+\Omega^2)\sum_{i=1}^{N}s_i\cos\beta_i+2\lambda\Omega\sum_{i=1}^{N}s_i\sin\beta_i\right]e^{\lambda t}, \tag{51b}$$

$$M=-m(l+r)\lambda^2e^{\lambda t}\sum_{i=1}^{N}s_i. \tag{51c}$$

Using Eqs. (24), (32), and (44), the absorber motions s_i are expressed using the phase index. Substitution of $s_i=e^{\mathrm{j}k\beta_i}$ into Eq. (51) and conversion to complex form yield

$$P_x=-\mathrm{j}\frac{m}{2}\left[(\lambda+\mathrm{j}\Omega)^2\sum_{i=1}^{N}e^{\mathrm{j}(k+1)\beta_i}-(\lambda-\mathrm{j}\Omega)^2\sum_{i=1}^{N}e^{\mathrm{j}(k-1)\beta_i}\right]e^{\lambda t}, \tag{52a}$$

$$P_y=-\frac{m}{2}\left[(\lambda+\mathrm{j}\Omega)^2\sum_{i=1}^{N}e^{\mathrm{j}(k+1)\beta_i}+(\lambda-\mathrm{j}\Omega)^2\sum_{i=1}^{N}e^{\mathrm{j}(k-1)\beta_i}\right]e^{\lambda t}, \tag{52b}$$

$$M=-m(l+r)\lambda^2e^{\lambda t}\sum_{i=1}^{N}e^{\mathrm{j}k\beta_i}. \tag{52c}$$

Using the property that $\sum_{i=1}^{N}e^{\mathrm{j}k\beta_i}=0$ for any integer k that is not a multiple of N, as proved in the Appendix, the moment in Eq. (52c) vanishes when $k\neq0$, and the forces in Eqs. (52a) and (52b) vanish when $k\neq1,N-1$. Thus, the net force and moment that the absorbers exert on the rotor both vanish for the absorber modes. This agrees with the result derived by Kim et al. [25] showing that a mode with phase index $k\neq0,1,N-1$ is a balanced mode, i.e., a mode with no net force or moment on the rotor. The net rotor moment is not balanced (zero) for the rotational modes, and the net rotor force is not balanced for the translational modes.

4. Stability

Gyroscopic systems often experience critical speeds where an eigenvalue vanishes, divergence instability (at least one positive real eigenvalue), and flutter instability (complex eigenvalues with positive real parts). Fig. 4 shows the natural frequency loci of the six-absorber CPVA system with the parameters given in Table 1 for varying rotor speed. Non-zero critical speeds occur between 7000 and 8000 rad/s. No divergence or flutter instability occurs for the systems shown in

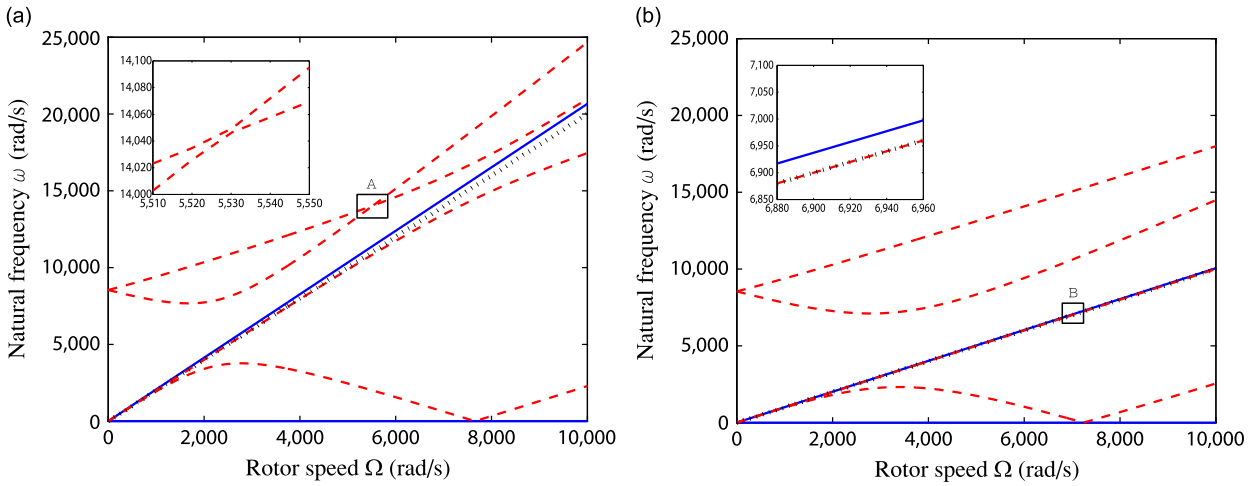

Fig. 4. Natural frequencies, ω (rad/s), of the systems with six equally spaced, identical absorbers and the system parameters given in Table 1 for varying rotor speed. Absorber modes are shown by dotted (black) lines, rotational modes are shown by solid (blue) lines, and translational modes are shown by dashed (red) lines. (a) Non-unity tuning. (b) Unity tuning. The inset figures zoom in on the highlighted regions A and B. (For interpretation of the references to color in this figure caption, the reader is referred to the web version of this article.)

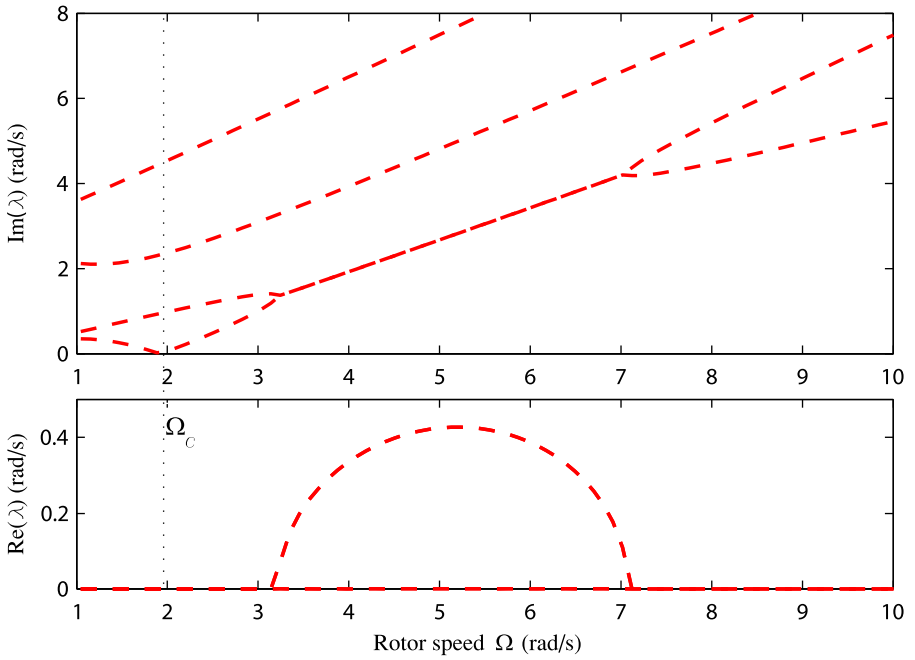

Fig. 5. Translational mode eigenvalues, λ (rad/s), of the system with six equally spaced, identical absorbers and the system parameters in Table 3 for varying rotor speed. The tuning order of 1/2 is less than unity.

Fig. 4. A critical speed near $\Omega = 2$ rad/s and flutter instability occur in Fig. 5 for the system with tuning order less than unity. These topics and numerical results are investigated below.

4.1. Critical speeds

No restrictions are imposed on the eigenvalues when deriving the vibration mode structure above, so the modal properties still hold at critical speeds where at least one eigenvalue vanishes. Substitution of $\lambda = 0$ into Eq. (15) yields

$$(\mathbf{K}_b - \Omega_c^2 \mathbf{K}_\Omega)\boldsymbol{\phi}_c = \mathbf{0}. \tag{53}$$

Eq. (53) is an eigenvalue problem that yields the critical speeds Ω_c.

For the absorber modes, the pair of eigenvalues is given in Eq. (37). These eigenvalues vanish only for $\Omega=0$. There are no non-zero absorber mode critical speeds.

One pair of rotational mode eigenvalues is given in Eq. (20), and these vanish only for $\Omega=0$. The other pair of rotational mode eigenvalues are zero at all speeds, and these are associated with the rigid body mode. These zero eigenvalues and the rigid body mode have no implications on system stability, so they are not considered in the critical speed analysis. Thus, there are no non-zero rotational mode critical speeds.

For non-zero rotor speeds, there is only one non-zero translational mode critical speed. To show this, we first substitute the eigenvector for the translational modes given by Eq. (25) into Eq. (53), giving

$$[k_r-\Omega_c^2(m_r+Nm)]x_r+\Omega_c^2 ms\sum_{i=1}^{N}e^{\mathrm{j}\beta_i}\sin\beta_i=0, \tag{54a}$$

$$\mathrm{j}[k_r-\Omega_c^2(m_r+Nm)]x_r-\Omega_c^2 ms\sum_{i=1}^{N}e^{\mathrm{j}\beta_i}\cos\beta_i=0, \tag{54b}$$

$$\left(-\mathrm{j}x_r+\frac{l}{r}s\right)=0. \tag{54c}$$

Eq. (54c) yields $x_r=-\mathrm{j}sl/r$. Hence the critical speed eigenvector becomes

$$\boldsymbol{\phi}_c=s\left(-\mathrm{j}\frac{l}{r},\frac{l}{r},0,e^{\mathrm{j}\beta_1},e^{\mathrm{j}\beta_2},\ldots,e^{\mathrm{j}\beta_N}\right)^T. \tag{55}$$

Use of $x_r=-\mathrm{j}sl/r$ and Eq. (27) in either Eq. (54a) or (54b) yields the only non-zero critical speed as

$$\Omega_c=\sqrt{\frac{k_r}{m_r+Nm\left(1+\frac{r}{2l}\right)}}. \tag{56}$$

Although the modal structure of CPVA systems shares similarities with planetary gear systems [18], the critical speed behavior differs. In planetary gear systems, all three mode types have critical speeds [26].

4.2. Flutter instability

Because of the matrix symmetries in Eq. (15), the inner products $\tilde{m}=\overline{\boldsymbol{\phi}}^T\mathbf{M}\boldsymbol{\phi}$ and $\tilde{k}=\overline{\boldsymbol{\phi}}^T(\mathbf{K}_b-\Omega^2\mathbf{K}_\Omega)\boldsymbol{\phi}$ are real, and $\mathrm{j}\tilde{g}=\Omega\overline{\boldsymbol{\phi}}^T\mathbf{G}\boldsymbol{\phi}$ is purely imaginary. Pre-multiplying Eq. (15) by $\overline{\boldsymbol{\phi}}^T$ yields

$$\tilde{m}\lambda^2+\mathrm{j}\tilde{g}\lambda+\tilde{k}=0. \tag{57}$$

The solutions of Eq. (57) are

$$\lambda_{1,2}=\frac{-\mathrm{j}\tilde{g}\pm\sqrt{-\tilde{g}^2-4\tilde{m}\tilde{k}}}{2\tilde{m}}. \tag{58}$$

Flutter instability occurs when an eigenvalue λ is complex with positive real part. This can only happen when one and only one of $\tilde{m}$ and $\tilde{k}$ is negative. Expansion of $\tilde{m}$ for a general eigenvector yields

$$\tilde{m}=(m_r+Nm)(|x_r|^2+|y_r|^2)+J_r|\mu_r|^2+m\sum_{i=1}^{N}|(l+r)\mu_r+s_i|^2-m\sum_{i=1}^{N}(\overline{x}_r s_i+x_r\overline{s}_i)\sin\beta_i+m\sum_{i=1}^{N}(\overline{y}_r s_i+y_r\overline{s}_i)\cos\beta_i. \tag{59}$$

$\tilde{m}$ is positive for the rotational and absorber modes where the first and last two terms vanish. For the translational modes, substitution of the eigenvector given by Eq. (25) into Eq. (59) gives

$$\tilde{m}=2(m_r+Nm)|x_r|^2+\mathrm{j}Nm(x_r\overline{s}-\overline{x}_r s)+Nm|s|^2=(2m_r+Nm)|x_r|^2+Nm|\mathrm{j}x_r+s|^2>0. \tag{60}$$

Hence, $\tilde{m}$ is positive for all mode types.

For positive $\tilde{m}$, flutter instability is possible only when $\tilde{k}$ is negative. For a general eigenvector

$$\tilde{k}=k_r|x_r|^2+k_r|y_r|^2-\Omega^2\left[(m_r+Nm)(|x_r|^2+|y_r|^2)-m\sum_{i=1}^{N}(\overline{x}_r s_i+x_r\overline{s}_i)\sin\beta_i\right.$$
$$\left.+m\sum_{i=1}^{N}(\overline{y}_r s_i+y_r\overline{s}_i)\cos\beta_i-m\frac{l}{r}\sum_{i=1}^{N}|s_i|^2\right]. \tag{61}$$

$\tilde{k}$ is non-negative for the rotational and absorber modes. Hence, $\lambda_{1,2}$ in Eq. (58) are purely imaginary for these modes, and they will never experience flutter instability. This is also shown by the purely imaginary rotational mode eigenvalue in Eq. (20) and the purely imaginary absorber mode eigenvalue in Eq. (37). Substitution of the translational mode eigenvector given by Eq. (25) into Eq. (61) gives an expression for $\tilde{k}$ in which the sign of $\tilde{k}$ depends on the modal displacements and

system parameters. Positive and negative values of $\tilde{k}$ are possible, so no translational mode flutter conclusions are possible at this point.

When the angular speed of the rotor is less than the non-zero translational mode critical speed, the rotor translational stiffness satisfies the following condition derived from Eq. (56)

$$k_r \geq \left[m_r + Nm\left(1+\frac{r}{2l}\right)\right]\Omega^2. \tag{62}$$

Substitution of this inequality and the translational mode eigenvector in Eq. (25) into Eq. (61) yields

$$\tilde{k} \geq \Omega^2 Nm\left(\frac{r}{l}|x_r|^2 + \mathrm{j}\bar{x}_r s - \mathrm{j}x_r\bar{s} + \frac{l}{r}|s|^2\right) = \Omega^2 Nm\left|\sqrt{\frac{r}{l}}x_r + \mathrm{j}\sqrt{\frac{l}{r}}s\right|^2 \geq 0. \tag{63}$$

Hence, $\tilde{k}$ remains non-negative for the translational modes when the rotor speed is less than the non-zero translational mode critical speed, and flutter instability cannot occur.

For speeds greater than the non-zero translational mode critical speed, negative $\tilde{k}$ is a necessary but not sufficient condition for flutter instability. The important quantity is $\Delta = -\tilde{g}^2 - 4\tilde{m}\tilde{k}$, where the necessary and sufficient condition for flutter is $\Delta > 0$. For the translational modes, the quantity $\tilde{g}$ is

$$\mathrm{j}\tilde{g} = -2\Omega[2\mathrm{j}(m_r + Nm)|x_r|^2 + Nm(\bar{x}_r s - x_r\bar{s})]. \tag{64}$$

Expanding Δ with the use of Eqs. (59), (61), and (64) for the translational modes gives

$$\Delta = -8k_r|x_r|^2[(2m_r+Nm)|x_r|^2 + Nm|\mathrm{j}x_r + s|^2] - 4\Omega^2N^2m^2|s|^4 + 4\Omega^2Nm\left(1-\frac{l}{r}\right)|s|^2[(2m_r+Nm)|x_r|^2 + Nm|\mathrm{j}x_r+s|^2]. \tag{65}$$

Δ given in Eq. (65) can be positive only when l/r is less than unity. Thus, flutter instability can only occur in system whose tuning order is less than unity. Although this is a necessary but not sufficient condition, a variety of numerical experiments suggest that flutter instability occurs in every system with tuning order less than unity.

Similar to planetary gear systems, only the translational modes can experience flutter instability [26]. No flutter conditions were derived in [26] for planetary gear systems.

5. Purely rotational systems

In most prior studies on CPVA systems, the rotor translation is not considered. The rotor has pure rotation in this case; the two translational coordinates x_r and y_r are zero. Thus, the first two rows and columns of Eq. (11) are ignored and x_r, y_r are omitted from $\mathbf{q}$.

For rotational modes, the properties remain the same, because the reduced eigenvalue problem in Eq. (18) is not affected.

No translational modes exist with this model. Because the non-zero critical speed and flutter instability are associated with the translational modes, these also do not occur.

For absorber modes, Eqs. (35a) and (35b) that govern the rotor translation are no longer relevant. This is also true for Eq. (40) derived from Eqs. (35a) and (35b), so the tuning order does not affect the modal properties. Eq. (35d) still gives the absorber mode eigenvalues as $\lambda = \pm\mathrm{j}\Omega n$. Eq. (35c) gives $N-1$ independent absorber mode eigenvectors. Thus, there is one pair of complex conjugate absorber modes with eigenvalue multiplicity $N-1$ for the purely rotational model. The phase indices of the absorber modes are $k = 1, 2, \ldots, N-1$ in such systems. The same kind of behavior occurs in purely rotational planetary gear systems [27].

Overall, there are two pairs of rotational modes and one pair of absorber modes with eigenvalue multiplicity $N-1$. The total number of rotational and absorber modes is $N+1$ complex conjugate mode pairs, equalling the number of degrees-of-freedom. Thus, the purely rotational system has only rotational and absorber modes.

6. Numerical examples

The natural frequencies of the CPVA systems with the parameters given by Table 1 are shown in Table 2. These are calculated from Eq. (15). Each natural frequency shown in Table 2 corresponds to a pair of complex conjugate eigenvalues. There are exactly two pairs of rotational modes. One of the two pairs of rotational modes is always the rigid body mode. The pair of non-zero rotational eigenvalues and the pair of absorber mode eigenvalues agree with Eqs. (20) and (37) using the parameters in Table 1. Four pairs of translational modes exist for both the non-unity and unity tuning cases. Each unity tuning case shown in Table 2 has a pair of translational mode eigenvalues degenerate with the pair of absorber mode eigenvalues. This pair of translational modes has zero translation of the rotor. The multiplicity of the absorber mode natural frequency is $N-3$. The above results match the analytical proofs of the modal properties.

Fig. 4 shows the natural frequency loci of the six-absorber non-unity and unity tuning systems with the parameters given in Table 1. There are no regions of flutter instability for these systems, because they have tuning orders greater than or equal to unity. This agrees with the analytical result.

Table 3
Parameters of a CPVA example, which contains flutter instability.

Parameter	Value
Rotor mass, m_r (kg)	11
Absorber mass, m (kg)	0.9
Distance between center and pivot, l (m)	0.01
Absorber radius, r (m)	0.04
Rotor translational stiffness, k_r (N/m)	100

As shown in Fig. 4, the only non-zero critical speeds are translational mode critical speeds at 7.65×10^3 rad/s for the non-unity tuning system and 7.24×10^3 rad/s for the unity tuning system. These values agree with those calculated by Eq. (56).

The two larger degenerate translational mode natural frequencies split at zero rotor speed with one increasing and the other decreasing. This is classical gyroscopic system behavior seen in axisymmetric spinning disks [28–30], spinning shafts [31], and disk–spindle systems [32,33]. The two vanishing degenerate translational mode natural frequencies also split at $\Omega=0$ (although this is hard to see), but both of them increase. This behavior is unusual. The two larger translational mode eigenvalues are $\lambda=\pm j8.54\times10^3$ rad/s at zero rotor speed for both the non-unity and unity tuning systems, which agree with the values calculated by Eq. (31).

The enlarged figure of region A in Fig. 4(a) shows that the two larger translational mode loci approach and veer away from each other near $\Omega=5530$ rad/s. The veering behavior shown in region A of Fig. 4(a) can be found in Fig. 4(b) if higher rotor speeds are plotted. The lowest translational mode locus and the rigid body rotational mode locus cross at the non-zero translational mode critical speed. These two examples suggest that the natural frequency loci of different mode types can cross while loci of the same mode type veer. Similar behavior occurs in planetary gear systems [34].

One translational mode locus of the unity tuning system shown in Fig. 4(b) overlaps with the absorber mode locus. This agrees with the analytical result that one pair of translational mode eigenvalues is degenerate with the pair of absorber mode eigenvalues for the unity tuning case. Although the non-rigid body rotational mode locus seems to overlap with the absorber mode locus as well, the enlarged figure of region B shows that they are separated. The absorber and non-rigid body rotational mode loci increase linearly with different slopes as the rotor speed increases for both the non-unity and unity tuning systems, as expected from Eqs. (20) and (37).

To have flutter instability, the system must have tuning order less than unity. Fig. 5 shows the eigenvalue loci of the six-absorber system with the parameters given in Table 3. The tuning order of this system is $n=1/2<1$. Only the eigenvalues of the translational modes are shown. No rotational and absorber modes experience flutter instability. Because the real and imaginary loci are symmetric about the rotor speed axis, only the positive parts are plotted. The imaginary parts of the two lowest translational mode eigenvalues coalesce at $\Omega=3.1$ rad/s and split at $\Omega=7.1$ rad/s. The real parts of these two eigenvalues are non-zero within this range. Therefore, one of these two translational modes experiences flutter instability in this speed range. The non-zero translational mode critical speed of this example system occurs near $\Omega=2$ rad/s. This agrees with the analytical result that flutter instability does not occur for rotor speeds less than the non-zero translational mode critical speed. Numerous numerical examples all showed flutter instability for every case of $n<1$, although the analytical proof only gives $n<1$ as only a necessary (but not sufficient) condition for flutter. The speed range in which flutter instability occurs becomes larger and moves to higher rotor speeds as the tuning order increases to unity from below.

7. Conclusions

This paper identifies and proves the natural frequency spectra and structured mode properties of the CPVA system with N equally spaced, identical absorbers. The cyclic symmetry of the CPVAs results in the well-defined modal structure. The CPVA system has only rotational, translational, and absorber modes. The vibration modes are complex-valued, and the phase differences between various degrees-of-freedom in each mode type are derived. The critical speeds and flutter instability conditions of the CPVA system are determined.

1. The rotational modes have pure rotation (no translation), and the translational modes have pure translation (no rotation) of the rotor. No rotor motion occurs for the absorber modes. For both the non-unity and unity tuning cases, there are two pairs of complex conjugate rotational modes, four pairs of complex conjugate translational modes, and one pair of complex conjugate absorber modes with eigenvalue multiplicity $N-3$. The absorber modes exist only when more than three absorbers are used.
2. A unique phase index is used to describe the phases between the degrees of freedom for the complex-valued modes. There is no overlap of phase indices between the three mode types. A mode with zero phase index (rotational mode) is a standing wave mode. Non-zero phase index indicates a traveling wave mode (translational and absorber modes).
3. The absorber motions in an absorber mode exert no net force or moment on the rotor. The absorbers exert a net rotor moment (but no force) for a rotational mode, and a net rotor force (but no moment) for a translational mode.
4. For the unity tuning case, a pair of complex conjugate translational modes has zero translation of the rotor for any rotor speed. The associated pair of eigenvalues is degenerate with the pair of absorber mode eigenvalues.

5. There is exactly one non-zero critical speed, and it is associated with a translational mode. Flutter instability can only occur in the translational modes and only for tuning orders less than unity. If it occurs, the flutter instability speed range is above the non-zero translational mode critical speed.

Acknowledgment

We thank Chris Cooley of the Ohio State University for his detail assistance reviewing all the work in this paper and his valuable suggestions, including to calculate the closed-form expressions of the eigenvalues from the characteristic equations and to contrast the real and complex-valued absorber modes in Eqs. (43) and (46).

Appendix A. Properties of equally spaced cyclic devices

The cyclic symmetry of equally spaced periodic devices possesses some unique geometric properties. The positions of N equally spaced devices mounted around a disk can be expressed by the angles $\beta_i = 2\pi(i-1)/N$, $i = 1, 2, \ldots, N$. The following proves that these angles satisfy

$$\sum_{i=1}^{N} e^{\mathrm{i}k\beta_i} = 0, \tag{A.1a}$$

$$\sum_{i=1}^{N} \cos^2 \beta_i = \sum_{i=1}^{N} \sin^2 \beta_i = \frac{N}{2}, \tag{A.1b}$$

$$\sum_{i=1}^{N} \sin \beta_i \cos \beta_i = 0, \tag{A.1c}$$

where k is any integer that is not a multiple of N.

Because k is not a multiple of N, $k \neq pN$ for any integer p. Applying trigonometric identities yields

$$\begin{aligned}\sin \frac{k\pi}{N} \sum_{i=1}^{N} \cos \frac{2k\pi i}{N} &= \sum_{i=1}^{N} \sin \frac{k\pi}{N} \cos \frac{2k\pi i}{N} = \sum_{i=1}^{N} \frac{1}{2}\left[\sin \frac{(2i+1)k\pi}{N} - \sin \frac{(2i-1)k\pi}{N}\right] \\ &= \frac{1}{2}\left[\sin \frac{(2N+1)k\pi}{N} - \sin \frac{k\pi}{N}\right] = \sin k\pi \cos \frac{(N+1)k\pi}{N} = 0.\end{aligned} \tag{A.2}$$

Similarly, $\sin(k\pi/N) \sum_{i=1}^{N} \sin 2k\pi i/N = 0$. Because $k \neq pN$, thus $\sin k\pi/N \neq 0$. This implies that for any integer $k \neq pN$,

$$\sum_{i=1}^{N} e^{\mathrm{i}k\beta_i} = \sum_{i=1}^{N} e^{\mathrm{i}2k\pi(i-1)/N} = \sum_{i=1}^{N} e^{\mathrm{i}2k\pi i/N} = \sum_{i=1}^{N} \cos \frac{2k\pi i}{N} + j \sum_{i=1}^{N} \sin \frac{2k\pi i}{N} = 0. \tag{A.3}$$

Trigonometric identities also give

$$\sum_{i=1}^{N} \cos^2 \beta_i + \sum_{i=1}^{N} \sin^2 \beta_i = \sum_{i=1}^{N} (\cos^2 \beta_i + \sin^2 \beta_i) = N, \tag{A.4a}$$

$$\sum_{i=1}^{N} \cos^2 \beta_i - \sum_{i=1}^{N} \sin^2 \beta_i = \sum_{i=1}^{N} (\cos^2 \beta_i - \sin^2 \beta_i) = \sum_{i=1}^{N} \cos 2\beta_i = \sum_{i=1}^{N} \cos \frac{4\pi i}{N} = 0. \tag{A.4b}$$

Hence,

$$\sum_{i=1}^{N} \cos^2 \beta_i = \sum_{i=1}^{N} \sin^2 \beta_i = \frac{N}{2}. \tag{A.5}$$

Also,

$$\sum_{i=1}^{N} \sin \beta_i \cos \beta_i = \frac{1}{2} \sum_{i=1}^{N} \sin 2\beta_i = \frac{1}{2} \sum_{i=1}^{N} \sin \frac{4\pi i}{N} = 0. \tag{A.6}$$

References

[1] E.S. Taylor, Crankshaft torsional vibration in radial aircraft engines, *S.A.E. Journal* 38 (3) (1936) 81–89.
[2] D.E. Newland, Nonlinear aspects of the performance of centrifugal pendulum vibration absorbers, *Journal of Engineering for Industry* 63-WA-275 (1964) 257–263.
[3] H.H. Denman, Tautochronic bifilar pendulum torsion absorbers for reciprocating engines, *Journal of Sound and Vibration* 159 (2) (1992) 251–277.

[4] C.-T. Lee, S.W. Shaw, The non-linear dynamic response of paired centrifugal pendulum vibration absorbers, *Journal of Sound and Vibration* 203 (5) (1997) 731–743.
[5] C.-T. Lee, S.W. Shaw, V.T. Coppola, A subharmonic vibration absorber for rotating machinery, *Journal of Vibration and Acoustics* 119 (4) (1997) 590–595.
[6] C.-P. Chao, S.W. Shaw, C.-T. Lee, Stability of the unison response for a rotating system with multiple tautochronic pendulum vibration absorbers, *Journal of Applied Mechanics* 64 (1) (1997) 149–156.
[7] A.S. Alsuwaiyan, S.W. Shaw, Performance and dynamic stability of general path centrifugal pendulum vibration absorbers, *Journal of Sound and Vibration* 252 (5) (2002) 791–815.
[8] C.-P. Chao, C.-T. Lee, S.W. Shaw, Non-unison dynamics of multiple centrifugal pendulum vibration absorbers, *Journal of Sound and Vibration* 204 (5) (1997) 769–794.
[9] C.-P. Chao, S.W. Shaw, The dynamic response of multiple pairs of subharmonic torsional vibration absorbers, *Journal of Sound and Vibration* 231 (2) (2000) 411–431.
[10] M. Albright, T. Crawford, F. Speckhart, Dynamic testing and evaluation of the torsional vibration absorber, *Motorsports Engineering Conference and Exposition*, Dearborn, MI, USA, 1994.
[11] T.M. Nester, P.M. Schmitz, A.G. Haddow, S.W. Shaw, Experimental observations of centrifugal pendulum vibration absorbers, *The 10th International Symposium on Transport Phenomena and Dynamics of Rotating Machinery*, no. ISROMAC10-2004-043, Honolulu, Hawaii, USA, 2004.
[12] A.G. Haddow, S.W. Shaw, Centrifugal pendulum vibration absorbers: an experimental and theoretical investigation, *Nonlinear Dynamics* 34 (3–4) (2003) 293–307.
[13] S.W. Shaw, P.M. Schmitz, A.G. Haddow, Tautochronic vibration absorbers for rotating systems, *Journal of Computational and Nonlinear Dynamics* 1 (4) (2006) 283–293.
[14] D.L. Cronin, Shake reduction in an automobile engine by means of crankshaft-mounted pendulums, *Mechanism and Machine Theory* 27 (5) (1992) 517–533.
[15] O.A. Bauchau, J. Rodriguez, S.-Y. Chen, Modeling the bifilar pendulum using nonlinear, flexible multibody dynamics, *Journal of the American Helicopter Society* 48 (1) (2003) 53–62.
[16] J. Lin, R.G. Parker, Analytical characterization of the unique properties of planetary gear free vibration, *Journal of Vibration and Acoustics* 121 (3) (1999) 316–321.
[17] T. Eritenel, R.G. Parker, Modal properties of three-dimensional helical planetary gears, *Journal of Sound and Vibration* 325 (1–2) (2009) 397–420.
[18] C.G. Cooley, R.G. Parker, Vibration properties of high-speed, gyroscopic planetary gears, *Journal of Vibration and Acoustics*, in press, http://dx.doi.org/10.1115/1.4006646.
[19] R. Monroe, S. Shaw, A. Haddow, B. Geist, Accounting for roller dynamics in the design of bifilar torsional vibration absorbers, *Journal of Vibration and Acoustics* 133 (6) (2011). 061002-1–10.
[20] L. Meirovitch, A new method of solution of the eigenvalue problem for gyroscopic systems, *AIAA Journal* 12 (10) (1974) 1337–1342.
[21] B.J. Olson, Order-tuned Vibration Absorbers for Systems with Cyclic Symmetry with Applications to Turbomachinery, PhD Thesis, Michigan State University, East Lansing, MI, 2006.
[22] H. Kim, I.Y. Shen, Ground-based vibration response of a spinning, cyclic, symmetric rotor with gyroscopic and centrifugal softening effects, *Journal of Vibration and Acoustics* 131 (2) (2009). 021007–1–13.
[23] B.J. Olson, S.W. Shaw, C. Pierre, Order-tuned vibration absorbers for cyclic rotating flexible structures, ASME International Design Engineering Technical Conferences, no. DETC2005-84641, Long Beach, CA, USA, 2005.
[24] G.S. Ottarsson, Dynamic Modeling and Vibration Analysis of Mistuned Bladed Disks, PhD Thesis, University of Michigan, Ann Arbor, MI, 1994.
[25] H. Kim, N.T. Khalid Colonnese, I.Y. Shen, Mode evolution of cyclic symmetric rotors assembled to flexible bearings and housing, *Journal of Vibration and Acoustics* 131 (5) (2009). 051008-1–9.
[26] C.G. Cooley, R.G. Parker, Mechanical stability of high-speed planetary gears, *International Journal of Mechanical Sciences*, submitted for publication.
[27] Y. Guo, R.G. Parker, Purely rotational model and vibration modes of compound planetary gears, *Mechanism and Machine Theory* 45 (3) (2010) 365–377.
[28] S.A. Tobias, R.N. Arnold, The influence of dynamical imperfection on the vibration of rotating disks, *Journal of Mechanical Engineering Science* 171 (1959) 669–690.
[29] C.D. Mote Jr., Stability of circular plates subjected to moving loads, *Journal of the Franklin Institute* 290 (4) (1970) 329–344.
[30] J.S. Chen, D.B. Bogy, Effects of load parameters on the natural frequencies and stability of a flexible spinning disk with a stationary load system, *Journal of Applied Mechanics* 59 (2) (1992) S230–S235.
[31] R.P.S. Han, J.W.-Z. Zhu, Modal analysis of rotating shafts: a body-fixed axis formulation approach, *Journal of Sound and Vibration* 156 (1) (1992) 1–16.
[32] R.G. Parker, P.J. Sathe, Free vibration and stability of a spinning disk–spindle system, *Journal of Vibration and Acoustics* 121 (3) (1999) 391–396.
[33] R.G. Parker, P.J. Sathe, Exact solutions for the free and forced vibration of a rotating disk–spindle system, *Journal of Sound and Vibration* 223 (3) (1999) 445–465.
[34] J. Lin, R.G. Parker, Natural frequency veering in planetary gears, *Mechanics of Structures and Machines* 29 (4) (2001) 411–429.